

Geochemical Characteristics of Mississippian to Pliensbachian Volcanic and Hypabyssal Rocks in the Hoodoo Mountain Area (NTS 104B/14E)

by A. Zagorevski¹, M.G. Mihalynuk² and J.M. Logan²

KEYWORDS: Hoodoo Mountain, Andrei Icefield, Andrei Glacier, Stikine assemblage, Stuhini Group, Hazelton Group, Iskut River, Twin Glacier River, whole-rock geochemistry

INTRODUCTION

Carboniferous to Jurassic rocks of the northwestern Stikinia commonly comprise thick successions of petrographically similar sedimentary, volcanoclastic and consanguineous hypabyssal rocks. The similarity of these sequences leads to ambiguity in correlations of units, hampering the establishment of a consistent stratigraphic framework in the predominantly ice and snow-covered Hoodoo Mountain area (NTS 104B/14; Figure 1). In addition, this part of Stikinia contains economically important, diverse and epoch specific metallotects that include; Carboniferous Kuroko type VHMS, Triassic Besshi type VMS, Triassic and Jurassic calcalkaline and alkaline Cu-Au-Ag±Mo porphyry, skarn and vein deposits and Jurassic submarine exhalative Au-Ag-rich VMS mineralization. The majority of these deposits are either stratabound or directly related to short-lived magmatic events making stratigraphic position a critical factor in understanding which deposit types are likely to be present. The purpose of this contribution is to test the utility of whole rock geochemistry to discriminate and calibrate the Mississippian to Pliensbachian stratigraphy proposed by Mihalynuk *et al.* (2011a; 2011b), thereby providing a means of directing cost effective and successful mineral exploration throughout the varied stratigraphy of the area.

REGIONAL STRATIGRAPHY

The Hoodoo Mountain area (NTS 104/14E; Figure 1) is underlain by rocks characteristic of northwestern Stikinia (Stikine terrane). In the adjacent areas, Stikinia comprises well-stratified, middle Paleozoic to early Mesozoic sedimentary, volcanic and plutonic rocks. The Early Devonian to Permian Paleozoic Stikine assemblage

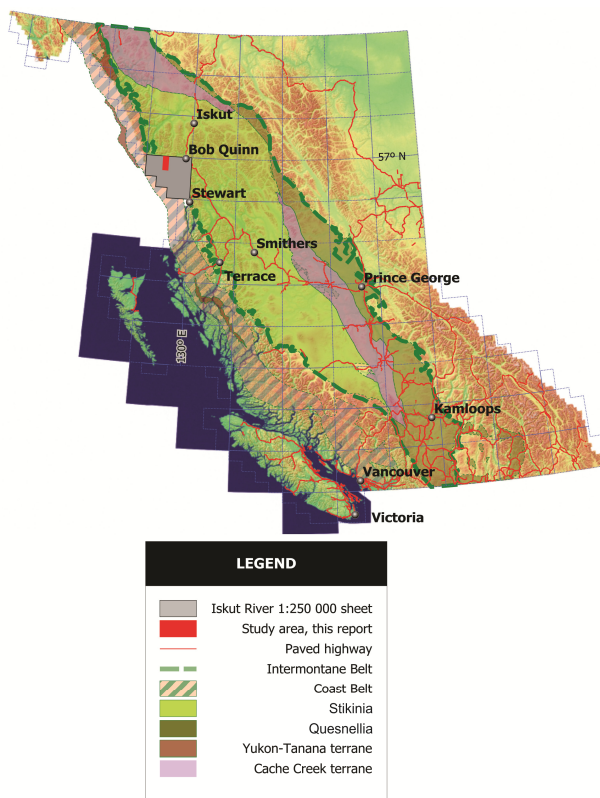


Figure 1. Location of the Iskut study area (red) shown within NTS 104B map sheet (grey), near the boundary of the Coast Belt and western Stikine terrane.

and Late Triassic Stuhini Group are overlain by the Early Jurassic Hazelton Group (Monger, 1977; Anderson, 1993; Logan *et al.*, 2000). In the Forrest Kerr area, the Stikine assemblage contains Lower to Middle Devonian strata (Read *et al.*, 1989), whereas equivalent rocks are unknown in the Hoodoo Mountain area. Both Carboniferous and Permian portions of the Stikine assemblage are characterized in part by carbonate units. The Carboniferous bimodal, volcano-sedimentary rocks are typically separated by a mid-Carboniferous carbonate that is characterized by locally abundant large crinoid columnals (Logan *et al.*, 2000). Up section, the Permian Stikine assemblage in the Hoodoo Mountain area is characterized by predominantly massive to bedded carbonate and chert layers, containing large and abundant rugosan horn corals and, locally, packstone with giant foraminifera. This contrasts with adjacent areas, where

¹ Geological Survey of Canada, Ottawa, ON

² British Columbia Geological Survey, Victoria, BC

This publication is also available, free of charge, as colour digital files in Adobe Acrobat® PDF format from the BC Ministry of Energy and Mines website at <http://www.empr.gov.bc.ca/Mining/Geoscience/PublicationsCatalogue/Fieldwork>.

volcaniclastic rocks are observed within the Permian section (Brown *et al.*, 1996; Logan *et al.*, 2000).

The Late Triassic Stuhini Group unconformably overlies the Stikine assemblage (Logan *et al.*, 2000), although this contact has not been directly observed in the eastern Hoodoo Mountain area. Stuhini Group strata can be broadly divided into two packages. The lower Stuhini Group strata are characterized by basinal shale, limestone and epiclastic volcanic rocks that grade into and are overlain by volcanic and conglomeratic rocks of the upper Stuhini Group. The upper Stuhini Group characteristically contains augite and feldspar porphyritic volcanic rocks, and polymictic conglomerate containing volcanic and plutonic derived clasts. A distinctive brown and orange-weathering, coarse biotite and K-feldspar-phyritic tuff and volcanogenic conglomerate is also believed to be Late Triassic (Norian) on the basis of dated subvolcanic intrusions (Newmount Lake property: Romios Gold Resources Inc., 2008) and correlation with similar rocks in the Galore Creek area (Logan and Koyanagi, 1994).

The Early to Middle Jurassic Hazelton Group overlies Stuhini Group strata above an angular unconformity (Henderson *et al.*, 1992; Brown *et al.*, 1996). McDonald *et al.* (1996) simplified the stratigraphy of the Hazelton Group in the Iskut area into lower (Early Jurassic) and upper (Early to Middle Jurassic) sequences. The lower sequence of the Hazelton Group includes a basal coarse clastic unit, overlain by andesitic to rhyolitic volcanic rocks that in turn are overlain by turbiditic siliclastic rocks. The age of the lower sequence is constrained by Hettangian to Upper Aalenian fossil collections and *ca.* 194-186 Ma U/Pb zircon ages (Macdonald *et al.*, 1996). The upper sequence is dominated by *ca.* 181-173 Ma (Childe *et al.*, 1994) bimodal volcanic rocks that occupy the Eskay rift of Alldrick *et al.* (2005) and Aalenian to Bajocian (?) fossil collections (Nadaraju, 1993). The age overlap between lower and the upper sequences reflects the regional continuity of the medial sedimentary unit and the discontinuous and diachronous nature of the upper rift volcanic sequence.

ANALYTICAL METHODS

Forty-four representative volcanic, epiclastic and intrusive samples were collected across the study area (Figure 2). Very few suitable lithologies were identified in the Jurassic section and as such, the Hazelton Group is underrepresented. Whole rock geochemistry samples of altered and non-altered rocks were screened to ensure internal homogeneity. The samples were trimmed with a diamond saw to remove veins and to minimize weathering. Major and trace elements were analyzed at Acme Laboratories using ICP-ES and ICP-MS following lithium metaborate/tetraborate fusion and nitric acid digestion (analytical code 4A4B). A summary of results is presented in Table 1. Full analytical dataset and background information is presented in Zagorevski *et al.*

(2011a).

GEOCHEMICAL SUITE DESCRIPTION AND RESULTS

Mississippian Stikine assemblage

Felsic volcanic rocks

The rhyolitic rocks comprise several volcanic types including massive flows, columnar jointed flows, tuff breccia and lapilli tuff. Lapilli tuff commonly contains altered tube pumice (Figure 3a) and flow-banded clasts. The rhyolite samples are quartz and feldspar glomeroporphyritic and contain abundant glass. U-Pb dating of two samples of rhyolite yielded *ca.* 340 Ma crystallization ages (Zagorevski *et al.*, 2012). Rhyolite is locally associated with jasperite and barite exhalite horizons that host finely laminated chalcopyrite mineralization (Mihalynuk *et al.*, 2011b).

Felsic volcanic rocks plot in the rhyolite and dacite fields on rock type discrimination plot (Figures 4a, b). They are characterized by light rare earth (LREE) and Th enrichment, and depletion of Nb on normal mid-ocean ridge basalt (N-MORB) normalized extended trace element plots (Figure 5a). They plot in volcanic arc field on tectonic discrimination plot (Figure 4c). The trace element profiles closely resemble other Early to Middle Carboniferous strata in adjacent areas (Gunning, 1997; Logan, 2004).

Mafic volcanic rocks

Mississippian pillowed mafic flows are sparsely to strongly vesicular. They are sparsely porphyritic and contain trachytic feldspar and, locally, pyroxene pseudomorphs. Ground mass is typically dominated by feldspar microlites (Figure 3b). Basalts are interlayered with bedded, graded and locally-sourced mafic pebble conglomerate. Contacts between the rhyolite and basalt units are conformable and interfingering.

Three samples of pillow basalt plot in the basalt field on the Nb/Y-Zr/Ti plot and in the andesite field on the Zr/TiO₂-SiO₂ plot, suggesting pervasive silicification (Figures 4a, b). Each sample has a distinct normalized extended trace element profile, suggesting that they form parts of several distinct mafic suites; however, all samples are characterized by LREE, Th enrichment and high-field strength element (HFSE) depletion characteristic of arc settings (Figure 5b). All samples plot in the volcanic arc tholeiite field on tectonic discrimination plot (Figure 4d). The normalized extended trace element profiles in part overlap other Early to Middle Carboniferous strata in adjacent areas (Figure 5b; Gunning, 1997; Logan, 2004).

Granite

An extensive granitoid that was interpreted to be Late Devonian to early Mississippian age (Verrett pluton: Logan *et al.*, 2000) extends into the Hoodoo Mountain

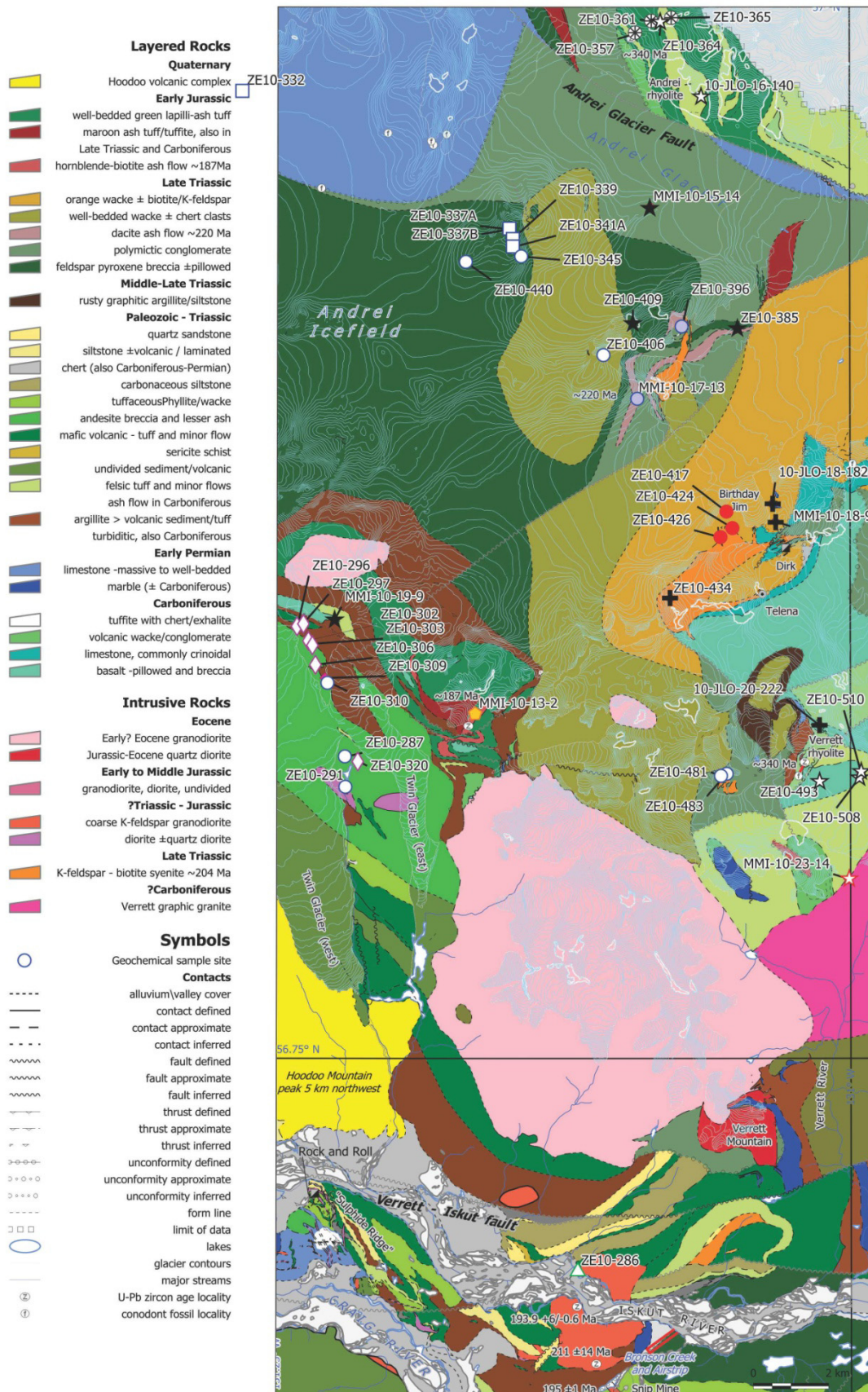


Figure 2. Geology of the Hoodoo Mountain area (from Mihalynuk *et al.*, 2011a). Whole-rock geochemistry sample locations utilize the same symbols as in Figure 4.

Table 1. Summary of geochemical data from NTS 104B/14E.

	Carboniferous												ITr						ITr or younger		eJr												
	Verette granite			basalt/andesite			rhyolite			basalt			Fs-porphyry			Cpx-porphyry			dacite			alkal tuff			alkal intrusive			hbl-dykes		dacite		Kfs granite	
	μ (3)	S.D.	μ (5)	S.D.	μ (6)	S.D.	μ (8)	S.D.	μ (5)	S.D.	μ (2)	S.D.	μ (3)	S.D.	μ (4)	S.D.	μ (5)	S.D.	μ (5)	S.D.	μ (5)	S.D.	μ (5)	S.D.	μ (5)	S.D.	μ (5)	S.D.	μ (5)	S.D.			
SiO2	76.76	56.68	5.19	74.16	3.71	54.38	5.21	49.54	2.67	48.80	1.34	66.64	1.17	46.18	7.61	47.67	2.59	50.43	1.66	61.86	60.09												
Al2O3	11.81	15.35	2.58	12.17	0.81	16.57	0.98	16.89	1.89	13.85	1.62	16.23	0.20	13.66	2.25	12.83	0.62	16.13	0.34	15.51	18.57												
Fe2O3	1.03	8.12	2.86	3.31	1.90	7.00	2.56	9.45	1.85	10.66	1.62	3.16	0.41	8.80	0.97	8.01	0.92	9.29	1.16	6.52	1.91												
MgO	0.21	2.75	1.34	1.24	0.59	4.67	3.44	5.47	1.68	7.83	1.35	1.52	0.06	3.33	2.54	4.17	2.60	4.91	0.69	1.47	0.45												
CaO	1.87	4.90	0.45	1.04	0.72	6.55	2.29	6.89	3.85	8.27	2.10	1.76	0.42	8.16	3.44	8.78	1.47	6.50	1.05	3.89	3.19												
Na2O	3.91	4.82	0.17	3.56	1.82	3.60	0.70	3.78	1.40	2.68	0.83	5.93	0.21	0.60	0.65	1.19	0.89	3.77	0.37	3.84	3.71												
K2O	1.64	1.28	1.07	2.17	2.73	2.06	2.08	2.25	1.34	2.18	0.35	2.61	0.05	8.72	1.82	7.39	2.23	3.68	1.43	3.03	6.99												
TiO2	0.16	1.15	0.22	0.30	0.19	0.93	0.28	0.94	0.10	0.82	0.08	0.36	0.03	0.61	0.20	0.70	0.14	1.56	0.47	0.64	0.39												
P2O5	0.03	0.71	0.52	0.07	0.05	0.34	0.10	0.33	0.09	0.34	0.06	0.15	0.03	0.44	0.05	0.64	0.06	0.33	0.09	0.19	0.14												
MnO	0.04	0.13	0.04	0.04	0.02	0.14	0.03	0.17	0.02	0.17	0.02	0.06	0.01	0.15	0.07	0.15	0.02	0.14	0.01	0.10	0.06												
Cr2O3	0.00	0.00	0.00	0.00	0.00	0.01	0.01	0.01	0.01	0.04	0.02	0.00	0.00	0.01	0.01	0.02	0.02	0.01	0.00	0.00	0.00												
Total	99.93	99.85	0.05	99.92	0.04	99.72	0.07	99.69	0.06	99.69	0.03	99.72	0.01	99.57	0.10	99.44	0.13	99.64	0.03	99.73	99.42												
LOI	2.50	3.97	1.78	1.86	1.02	3.48	1.62	3.96	1.71	3.02	0.73	2.30	0.14	8.93	6.91	7.90	1.63	2.88	0.52	2.70	3.90												
Ba	494	280	29	423	330	799	585	888	412	563	101	1369	60	2004	387	2930	860	1253	303	1502	4106												
Cs	3.20	0.33	0.06	0.46	0.53	5.17	10.57	3.59	2.89	0.56	0.27	0.85	0.49	3.30	1.56	2.78	2.67	0.28	0.16	0.90	2.00												
Hf	3.80	1.97	1.14	3.34	0.74	2.83	0.88	2.36	0.91	1.64	0.15	2.95	0.35	1.97	0.32	2.00	0.14	2.70	0.49	2.40	2.60												
Nb	3.40	1.83	1.25	2.68	0.47	6.60	2.27	5.64	3.68	2.86	0.52	3.55	0.07	9.93	4.71	10.88	0.85	7.14	1.00	4.40	6.30												
Pb	5.20	1.97	0.85	1.32	0.68	2.70	4.22	4.78	6.05	1.40	0.54	5.75	4.45	4.63	2.82	9.30	5.39	3.76	2.55	2.30	3.00												
Rb	28.9	11.7	8.1	20.0	20.7	44.3	55.7	49.6	30.3	34.9	16.5	43.3	11.6	180.0	60.5	126.5	48.8	48.6	18.5	88.6	157.2												
Sr	58	239	122	142	117	584	214	517	232	462	33	801	72	753	424	883	329	668	77	508	863												
Th	3.90	1.13	0.85	3.24	1.90	3.72	1.78	2.91	2.47	1.30	0.35	2.55	0.21	2.90	0.90	3.45	0.37	5.44	4.10	5.30	5.10												
U	2.00	0.70	0.46	1.38	0.48	1.53	0.63	1.29	1.00	0.70	0.16	1.50	0.14	1.43	0.15	1.58	0.13	1.88	1.52	2.50	6.00												
Y	38.50	44.53	23.06	31.24	9.61	21.97	2.69	19.90	3.31	17.18	1.49	9.15	0.49	13.87	1.97	14.88	2.38	18.62	1.71	14.50	12.90												
Zr	120	55	30	105	27	105	38	90	44	59	7	95	17	79	10	68	10	94	22	94	83												
La	6.80	13.13	9.72	10.26	5.54	19.32	5.19	14.16	6.35	7.78	1.50	12.15	0.21	13.13	5.20	15.83	1.14	18.42	4.54	14.80	25.30												
Ce	17.40	26.87	16.10	23.14	11.61	39.00	9.74	30.03	11.76	18.24	3.40	24.45	0.07	27.17	11.00	31.20	2.06	38.84	7.70	29.80	39.30												
Pr	2.46	4.34	2.72	3.08	1.43	4.88	1.07	3.75	1.13	2.47	0.40	3.11	0.24	3.11	1.23	3.60	0.30	5.07	0.76	3.29	4.33												
Nd	12.00	21.73	12.33	13.68	6.39	20.62	3.72	16.08	3.73	11.84	1.52	13.30	1.13	13.00	4.59	15.43	1.09	22.62	3.61	13.20	16.80												
Sm	3.48	5.89	3.41	3.58	1.59	4.09	0.37	3.68	0.58	2.91	0.28	2.57	0.13	2.70	0.86	3.14	0.31	4.64	0.39	2.79	3.24												
Eu	0.65	1.88	0.71	0.84	0.45	1.38	0.07	1.14	0.29	0.95	0.08	0.77	0.02	0.85	0.23	0.96	0.09	1.42	0.10	0.82	1.06												
Gd	4.67	7.51	4.32	4.24	1.81	4.07	0.45	3.67	0.41	3.21	0.22	2.12	0.04	2.65	0.57	3.05	0.30	4.30	0.45	2.75	2.83												
Tb	0.93	1.29	0.75	0.78	0.31	0.67	0.08	0.61	0.08	0.53	0.03	0.31	0.01	0.42	0.08	0.47	0.07	0.65	0.05	0.43	0.43												
Dy	5.85	7.88	4.57	4.88	1.75	3.75	0.52	3.38	0.45	2.98	0.14	1.54	0.08	2.38	0.47	2.57	0.42	3.36	0.25	2.49	2.29												
Hb	1.36	1.67	0.97	1.09	0.35	0.76	0.11	0.71	0.10	0.63	0.05	0.29	0.01	0.51	0.05	0.52	0.09	0.67	0.09	0.50	0.47												
Er	4.12	4.89	2.94	3.40	1.01	2.24	0.29	2.07	0.33	1.75	0.12	0.83	0.01	1.55	0.25	1.47	0.26	1.84	0.26	1.47	1.35												
Tm	0.64	0.75	0.46	0.55	0.16	0.34	0.04	0.31	0.05	0.27	0.02	0.13	0.00	0.23	0.02	0.23	0.04	0.27	0.04	0.23	0.22												
Yb	4.24	4.62	2.92	3.69	1.00	2.12	0.23	2.02	0.35	1.69	0.18	0.85	0.03	1.50	0.21	1.50	0.25	1.76	0.26	1.55	1.51												
Lu	0.67	0.69	0.42	0.57	0.15	0.32	0.04	0.31	0.06	0.26	0.03	0.13	0.00	0.23	0.03	0.23	0.03	0.26	0.04	0.25	0.25												

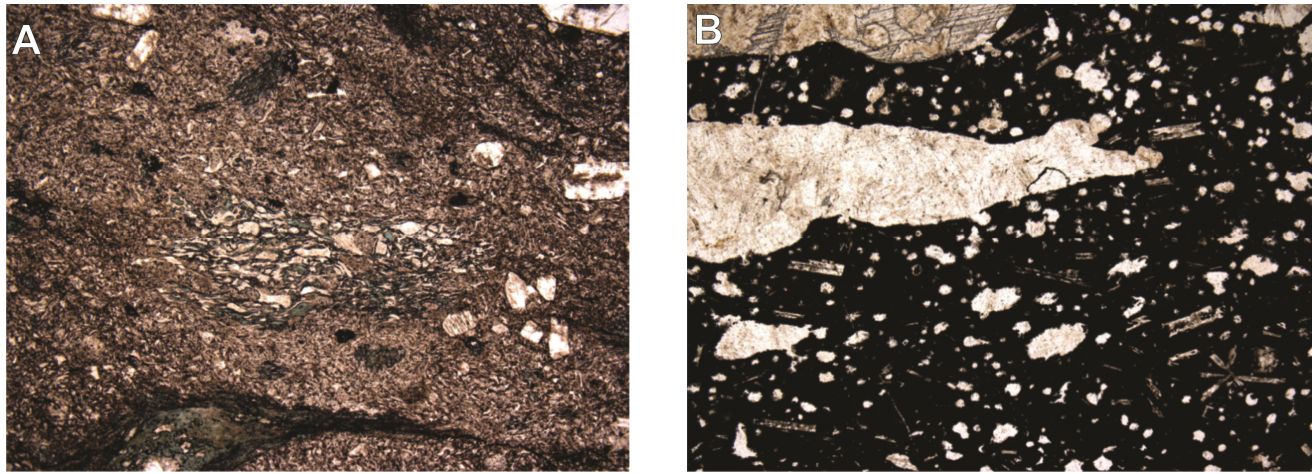


Figure 3. Representative photomicrographs of Mississippian units. A) Rhyolite lapilli tuff with altered (tube) pumice clast (FOV 7 mm). B) Trachytic basalt with large carbonate-filled pipe vesicles (FOV 3.5 mm).

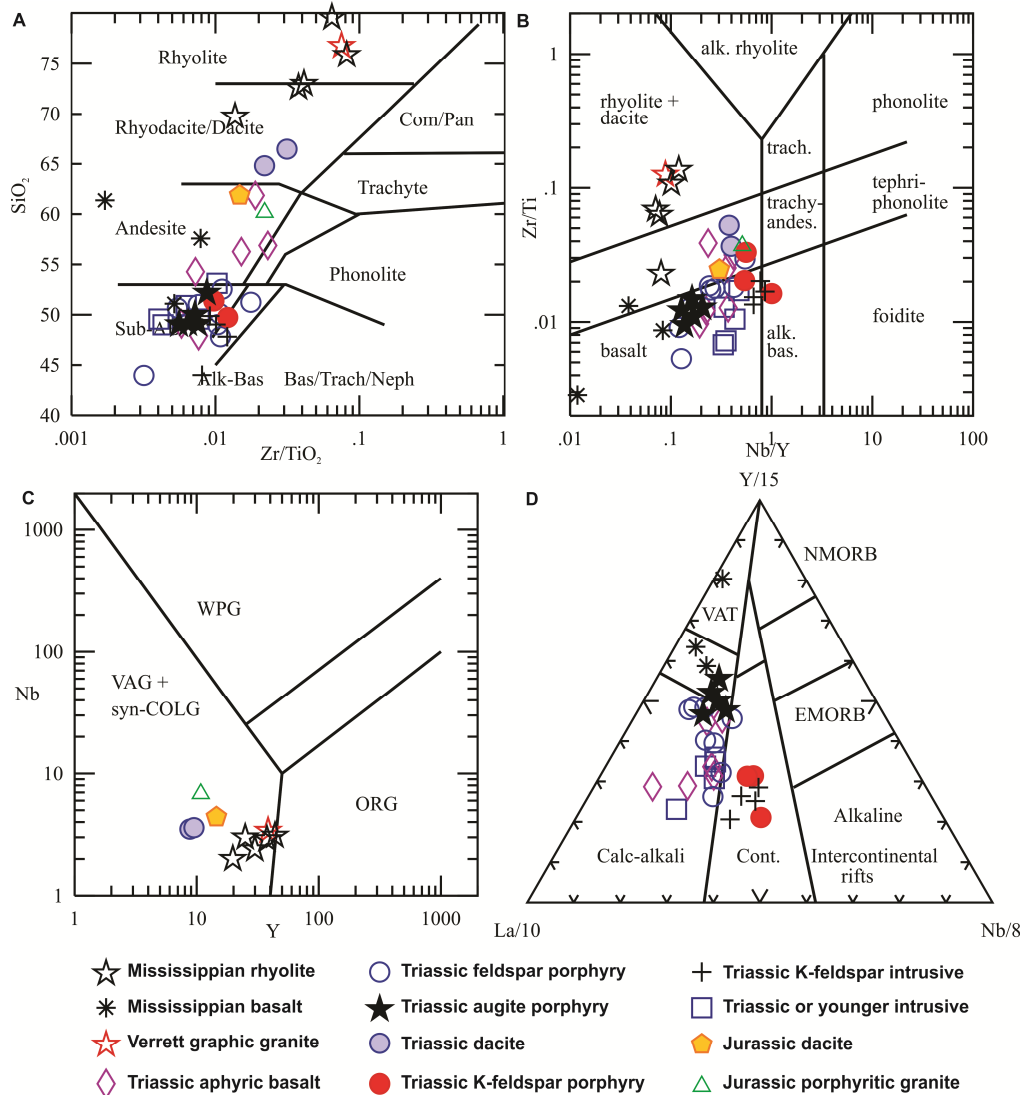


Figure 4. Rock type and tectonic discrimination plots of major units in the Hoodoo Mountain area (Winchester and Floyd, 1977; Pearce *et al.*, 1984; Cabanis and Lecolle, 1989; Pearce, 1996).

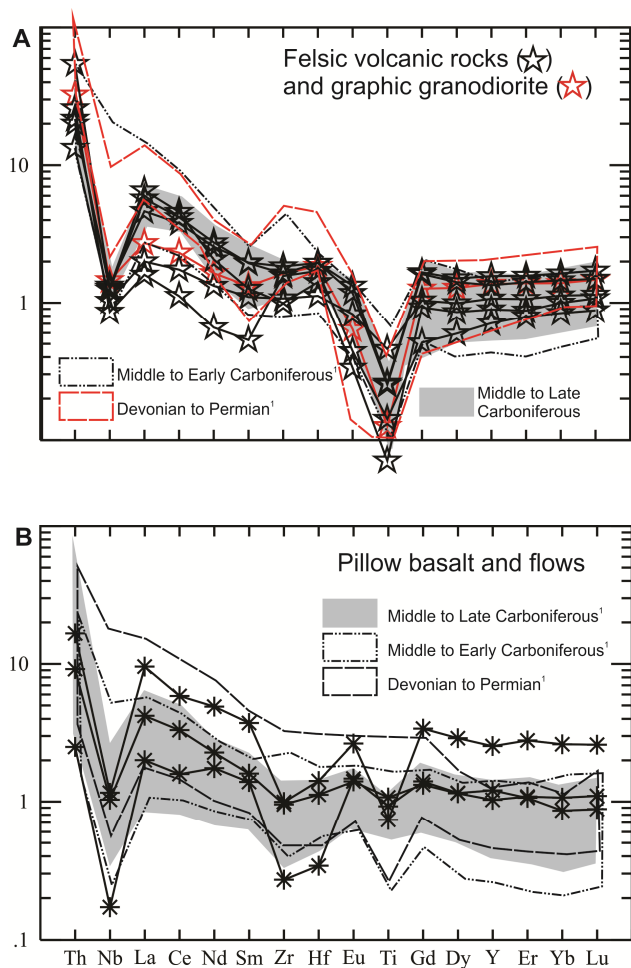


Figure 5. Trace element profiles of Mississippian rocks (N-MORB normalization from Sun and McDonough, 1989; ¹Gunning, 1997).

area (Figure 2), where it comprises predominantly cream to orange-coloured, medium to coarse grained, graphic leucogranite (see Figure 19 in Mihalynuk *et al.*, 2011b). An attempt to date the granite failed to yield any zircon (R. Friedman, personal communication, 2011). Since it appears to intrude dated Carboniferous strata in the study area, it has been reinterpreted to be Carboniferous or younger (Mihalynuk *et al.*, 2011b).

Geochemistry of the granite sample shows LREE, Th enrichment and Nb depletion on N-MORB normalized extended trace element plots (Figure 5a). It plots in the volcanic arc field on tectonic discrimination plots (Figure 4c). The trace element profile closely resembles Early to Middle Carboniferous volcanic rocks in the Hoodoo Mountain and adjacent areas.

Triassic Stuhini Group

The Triassic Stuhini Group is the most spatially extensive Mesozoic unit in the eastern Hoodoo Mountain area. The Stuhini Group is divided into five petrographically distinct volcanic units: aphyric basalt, feldspar porphyry, augite porphyry, dacite, and K-feldspar porphyry (Figures 6, 7). In general, each petrographic type is spatially restricted; suggesting that they belong to

different magmatic centres or were erupted at different times. The dacite unit has a U-Pb crystallization age of ca. 223 Ma (Zagorevski *et al.*, 2012). Ar/Ar geochronology and fossil identification to constrain the stratigraphic order for the remaining units is ongoing.

Aphyric basalt

A nunatak to the north of Twin Glaciers preserves a thick sequence of basaltic volcanic, hypabyssal, and epiclastic rocks. The volcanic rocks include aphyric to very sparsely feldspar porphyritic, variably amygdaloidal massive flows, lapilli tuff and tuff breccia (Figure 6a). The hypocristalline groundmass is dominated by felty to trachytic plagioclase microlites. Amygdales range from finely disseminated throughout the groundmass to large elongate pipe vesicles. Interlayered epiclastic rocks comprise locally-derived sandy to conglomeratic mafic turbidite. They are locally associated with calcareous wacke, fossiliferous shale, fossiliferous sandstone and chert.

Three samples of tuff breccia, two samples of massive flows and one sample of diabase plot in basalt and andesite fields on rock type discrimination diagrams (Figures 4a, b). All samples are characterized by LREE, Th enrichment and Nb, Ti depletion characteristic of arc settings (Figure 8a). In contrast to the Carboniferous mafic rocks (Figure 5), Nb is enriched relative to HREE, suggesting an enriched source. All samples plot in the calcalkaline field on tectonic discrimination plot (Figure 4d). The normalized extended trace element profiles overlap Late Triassic basalts in adjacent areas (Figure 8a; Brown *et al.*, 1996; Gunning, 1997).

Feldspar-porphyry

The feldspar porphyritic rocks include lapilli tuff and tuff breccia that are dominated by feldspar phenocrysts with lesser clinopyroxene and minor amphibole. Trachytic textures are common. Amphibole is observed in some samples where it is xenocrystic and clearly derived from cognate or accidental (Wright *et al.*, 1980) hornblende-diorite fragments (Figure 6b). Some blocks display trachytic feldspars with hornblende phenocrysts set in a glassy matrix (Figure 6b), indicating that some hornblende-porphyritic magma cooled rapidly. Ar/Ar analysis of a sample of hornblende from this unit is pending.

Eight samples of feldspar-porphyritic tuff and hypabyssal intrusive rocks were selected for analysis. Samples with visible xenoliths and xenocrysts were not analyzed to minimize the risk of contamination. Single volcanic fragments were collected where possible from breccias to minimize the effect of contamination and mixing of multiple lithologies. All eight samples plot in the basalt field on the rock type discrimination diagrams (Figures 4a, b). Similar to the aphyric basalt, all samples are characterized by LREE, Th enrichment and Nb, Ti depletion characteristic of arc settings (Figure 8b). All

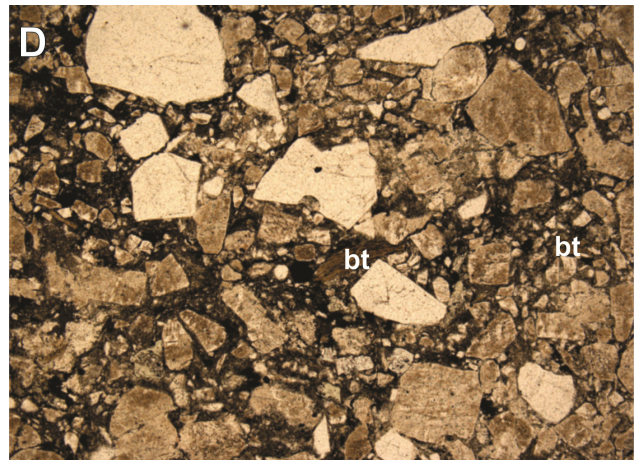
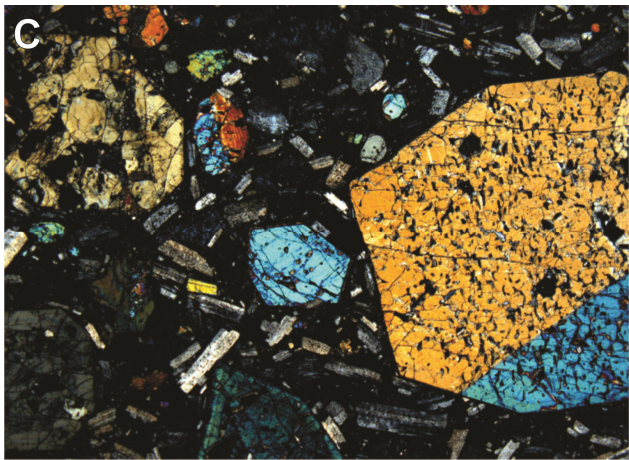
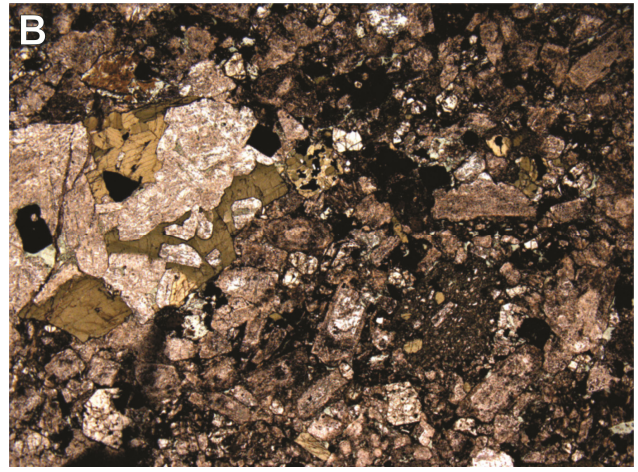
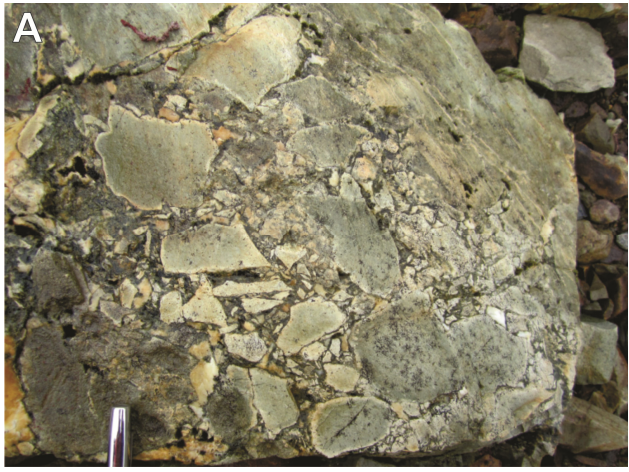


Figure 6. Representative photos and photomicrographs of Triassic calcalkaline units. A) Aphyric basalt tuff breccia (8 mm pen tip for scale). B) Feldspar porphyritic tuff with accidental gabbro clasts and hornblende xenocrysts and trachytic hornblende–feldspar lapilli (FOV 7 mm). C) Augite porphyry with sieve textured pyroxene crystals (FOV 7 mm). D) Dacite tuff with altered biotite (FOV 3.5 mm).

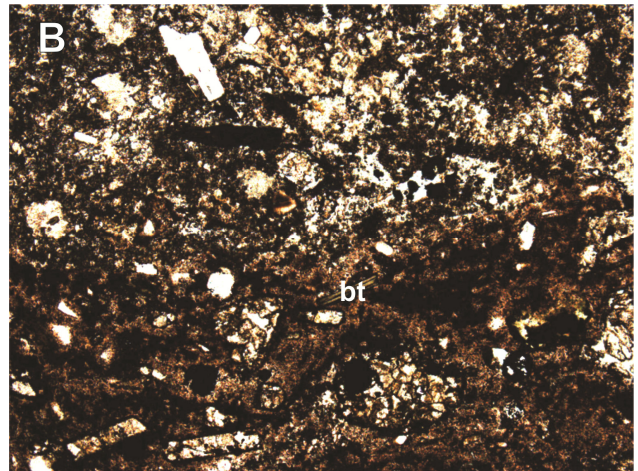
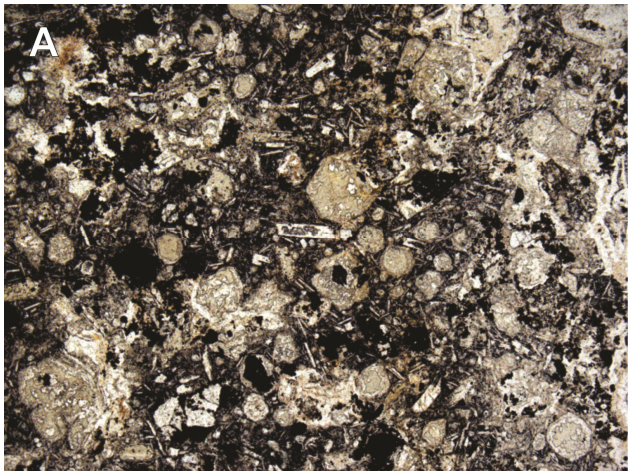


Figure 7. Representative photomicrographs of Triassic alkaline units. A) Spherical pseudomorphs suggest presence of altered leucite (FOV 3.5 mm). B) Lapilli tuff with characteristic biotite porphyritic lapilli (FOV 3.5 mm).

samples plot in the calcalkaline field on tectonic discrimination plot (Figure 4d). The normalized extended trace element profiles overlap Late Triassic feldspar-porphyrific andesites in adjacent areas (Figure 8b; Brown *et al.*, 1996; Gunning, 1997).

Augite porphyry

Augite porphyritic rock samples include lapilli tuff, tuff breccia, flows and sills. They are dominated by coarse clinopyroxene phenocrysts and subordinate to equally abundant amounts of feldspar phenocrysts. Coarse clinopyroxene crystals are commonly sieve-textured and contain thin, inclusion-free, coherent rims (Figure 6c). Medium to fine grained augite crystals also contain evidence of resorption followed by attainment of equilibrium with the melt.

Five samples of augite porphyry plot in the basalt field on the rock type discrimination plots (Figures 4a, b). Similar to the aphyric and feldspar-phyric basalts, all samples are characterized by LREE, Th enrichment and Nb, Ti depletion characteristic of arc settings (Figure 8c). All samples plot in the transitional area between volcanic arc tholeiite and calcalkaline basalt fields on tectonic discrimination plot (Figure 4d). The normalized extended trace element profiles overlap Late Triassic augite-porphyrific basalt in adjacent areas (Figure 8c; Brown *et al.*, 1996; Gunning, 1997).

Dacite

Triassic dacitic rocks comprise hypabyssal and extrusive quartz-feldspar porphyry and related crystal-rich tuffaceous rocks that occupy a thick package of cobble to boulder polymictic volcanic conglomerate. Crystal tuffs commonly contain minor biotite and accessory titanite. One sample yielded *ca.* 223 Ma U/Pb zircon age (Zagorevski *et al.*, 2012).

Two samples of dacite tuff were analyzed and they display LREE, Th enrichment and Nb depletion on N-MORB normalized extended trace element plots (Figure 8d). They plot in the volcanic arc field on tectonic discrimination plot (Figure 4c). Their trace element profile is distinctly more depleted in HREE as compared to the Early to Middle Carboniferous felsic volcanic rocks and Triassic dacite in adjacent areas (Figure 8d, Gunning, 1997).

K-feldspar porphyritic rocks

The K-feldspar porphyritic rocks appear to be restricted to isolated volcanic centres and comprise volcanic breccias/diatremes that are intercalated with rusty-weathering siliciclastic sediments and consanguineous K-feldspar porphyritic syenitic intrusive rocks. Potassium feldspar megacrystic intrusive rocks that mark these centres are locally affected by intense calcsilicate alteration and locally the volcanic, volcanoclastic and hypabyssal rocks host precious and base metal mineralization (Chadwick and Close, 2009).

Some units contain distinctive, 0.5 to 3 cm round pseudomorphs after leucite (Figure 7a). Others contain primary biotite, pyroxene and/or amphibole that are typically strongly altered or completely pseudomorphed (Figure 7b). Most of the samples are feldspathoid (leucite±nepheline) normative.

Three samples of fragments from a tuff breccia were analyzed. They plot near the boundary between sub-alkaline and alkaline basalt (Figures 4a, b). All samples are characterized by LREE, Th enrichment; however, in contrast to other Late Triassic basalts, Nb is only slightly depleted relative to La (Figure 8e). All plot in the continental rift field on tectonic discrimination plot (Figure 4d). The normalized extended trace element profiles overlap Late Triassic (Norian) feldspar-porphyrific basalt in adjacent areas (Gunning, 1997). Four samples of intrusive rocks overlap the volcanic rocks on tectonic discrimination and extended trace element plots (Figures 4d, 8e). All samples geochemically overlap the alkaline Zippa Mt. pluton melanosenite and syenite (Figure 8e).

Late Triassic or younger

Triassic or younger hornblende-bearing mafic dikes are concentrated in a dike complex in the central part of the field area (Figure 2). The variegated dikes have a sheeted appearance (*i.e.*, dike-in-dike) and range from hornblende-pyroxene phyric hypocrystalline to hornblende-plagioclase pegmatites (see Figure 21 in Mihalynuk *et al.*, 2011b). All varieties contain brown hornblende needles and prisms. Locally, fine-grained dikes are hornblende and pyroxene porphyritic (Figure 9a). Ar-Ar hornblende age results are pending for several samples of this unit.

Five dikes were sampled at different localities. Analyses of all the dikes display LREE and Th enrichment and Nb, Ti depletion characteristic of arc settings (Figure 8f). All samples plot in the calcalkaline field on tectonic discrimination plot (Figure 4d). The normalized extended trace element profiles overlap Late Triassic volcanic rocks in the study and adjacent areas.

Jurassic Hazelton Group

Hornblende and plagioclase porphyritic volcanoclastic rocks are locally common and characterize the Jurassic strata in the study area. A *ca.* 187 Ma U-Pb zircon crystallization age (Zagorevski *et al.*, 2012) from oxyhornblende-phyric, sparse quartz-eye dacite ash flow tuff constrains these rocks to the top of the lower sequence of the Hazelton Group (Macdonald *et al.* 1996). This tuff is interlayered with quartz-bearing, turbiditic volcanic sandstone, conglomerate, massive to bedded maroon to bright green tuff and lapilli tuff (Figure 9b).

A sample of Jurassic dacite tuff is characterized by LREE and Th enrichment, and Nb depletion on a N-MORB normalized extended trace element plot Figure 10a). It plots in the volcanic arc field on tectonic

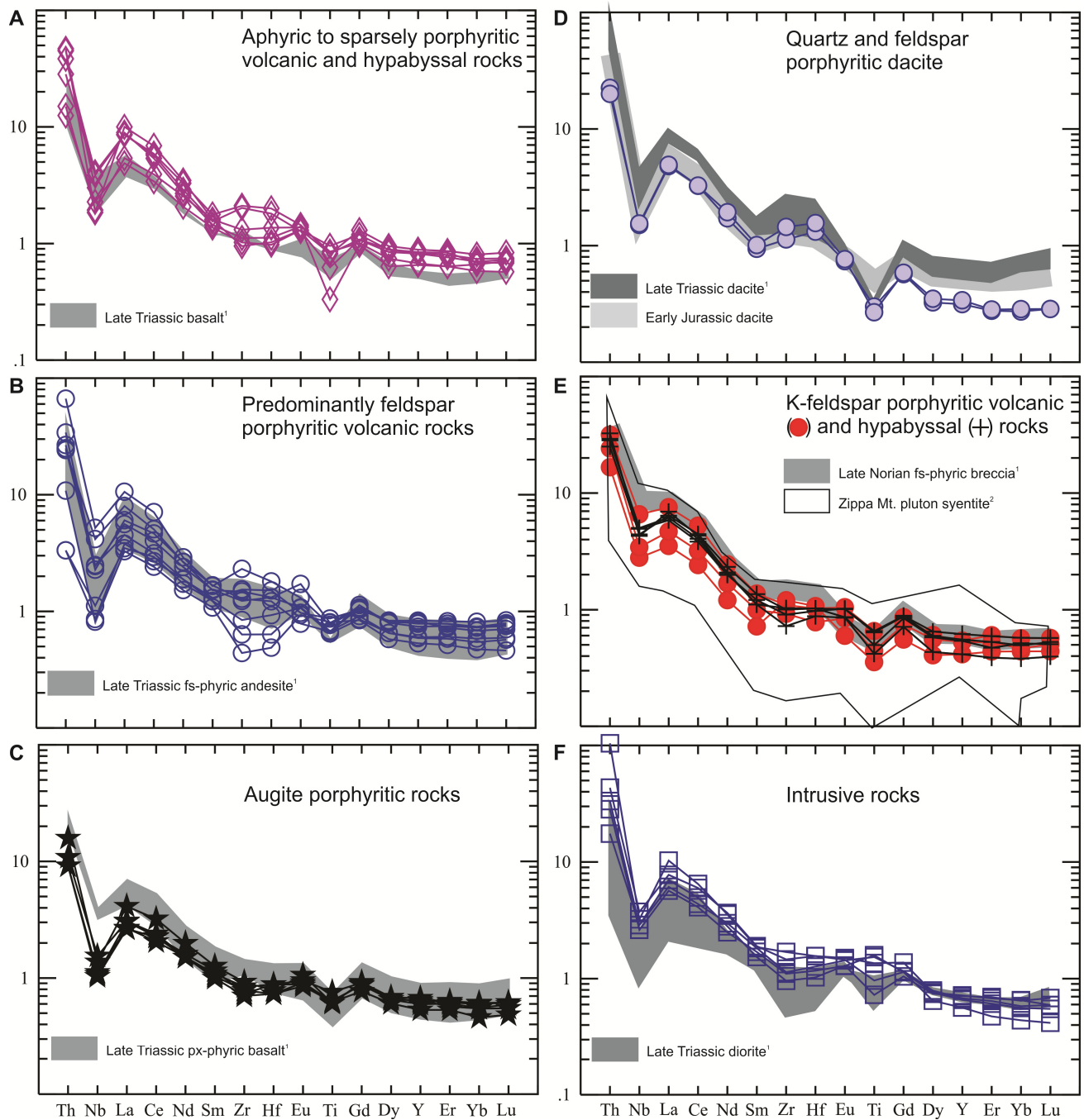


Figure 8. Trace element profiles of Triassic rocks (N-MORB normalization from Sun and McDonough, 1989; ¹Gunning, 1997; ²Coulson *et al.*, 1999).

discrimination plot (Figure 4c). The trace element profile is distinctly more depleted in HREE compared to the Early Carboniferous and Middle Jurassic volcanic rocks in the Hoodoo Mountain and adjacent areas (Figures 5a, 10a). From a geochemical perspective, the Jurassic dacite tuff is chemically similar to the Late Triassic dacite in the study and adjacent areas (Figure 10a).

Early Jurassic K-feldspar porphyry

A small, coarsely K-feldspar porphyritic to megacrystic monzogranite pluton occurs along the Iskut River Valley (Figure 2; Iskut Mass of Kerr, 1948). The pluton previously yielded discordant and uncertain U/Pb zircon crystallization ages of between 225 and 197 Ma (Macdonald *et al.*, 1992), but a concordant *ca.* 196 Ma age has been recently obtained (Zagorevski *et al.*, 2012).

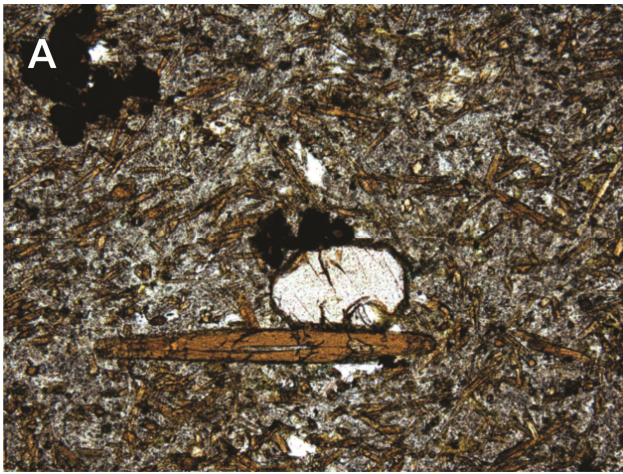


Figure 9. A. Photomicrograph of Triassic or younger hornblende porphyritic dike (FOV 1.75 mm). B) Jurassic dacitic tuff.

The K-feldspar porphyry contains quartz, distinguishing it from the Norian K-feldspar porphyritic rocks. One sample displays LREE and Th enrichment and Nb depletion on a N-MORB normalized extended trace element plot (Figure 10b). It plots in the volcanic arc field on tectonic discrimination plot (Figure 4c).

DISCUSSION

The Paleozoic to Mesozoic volcano-sedimentary and consanguineous plutonic rocks of the Hoodoo Mountain area are assigned to the Early Carboniferous to Permian Paleozoic Stikine assemblage, Late Triassic Stuhini Group and the Early Jurassic Hazelton Group on the basis of lithology and limited age dating. Whereas some lithologic characteristics of these units are unique (see previous also Logan *et al.*, 2000; Mihalynuk *et al.*, 2011b), they commonly contain indistinct lithologies complicating stratigraphic correlations in poorly exposed or constrained area. Whereas isotopic age dating can provide unique solutions, it is expensive. Here we utilize whole rock geochemical analyses from rocks in the Hoodoo Mountain area to test the utility of geochemistry in stratigraphic correlation and to identify the geochemical fingerprints of mineralized sequences.

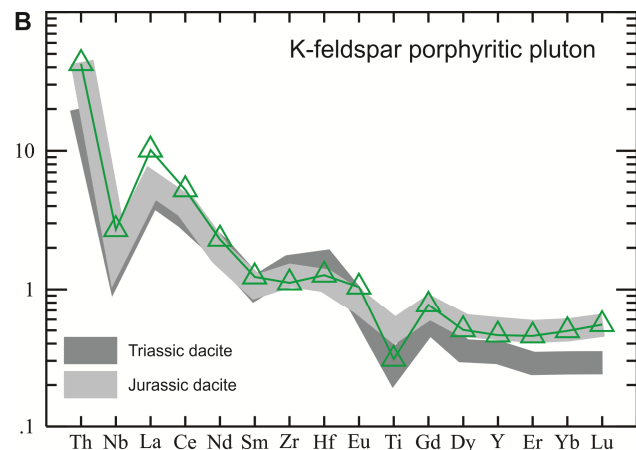
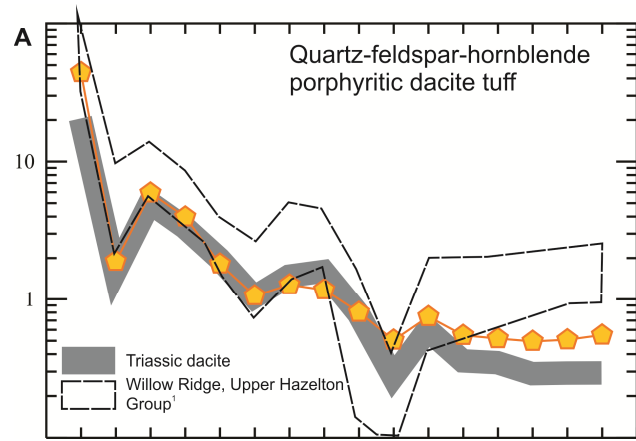


Figure 10. Trace element profile of Jurassic dacite and Jurassic monzodiorite (N-MORB normalization from Sun and McDonough, 1989; Barresi and Dostal, 2005).

Mississippian Stikine assemblage

Volcanic rocks of the Mississippian Stikine assemblage (Monger, 1977) include rhyolite and pillow basalt that host VMS-style mineralization (Logan *et al.*, 2000; Logan, 2004; Mihalynuk *et al.*, 2011b). The geochemical characteristics of both felsic and mafic rocks indicate a volcanic arc setting as previously proposed by many authors (*e.g.* Logan *et al.*, 2000; Logan, 2004). Rhyolitic rocks have low La/Yb(n) ratios characteristic of VMS-prospective tholeiitic FIII rhyolites (Lesher *et al.*, 1986). The Verrett graphic granite in the east part of the mapped area (Figure 2) has indistinguishable geochemical characteristics and is interpreted to form a subvolcanic pluton to the Mississippian arc. Regionally, the Mississippian Stikine assemblage is geochemically distinct from the Late Triassic and Early Jurassic rocks (see following); however, felsic rocks are geochemically similar to the VMS-prospective Middle Jurassic strata of the Eskay rift (Alldrick *et al.*, 2005; Barresi and Dostal, 2005), indicating occurrence of similar supra-subduction zone environments (*i.e.* nascent arc, back arc, arc rift) of different ages.

Triassic Stuhini Group

Late Triassic Stuhini Group can be subdivided into five petrographically distinct volcanic and hypabyssal units. Overall, the petrographic characteristics may be a useful stratigraphic marker pending further age investigations. Generally, the aphyric basalt, feldspar porphyry and augite porphyry have similar trace element chemistry. All of the calcalkaline rocks have similar LREE, Th enrichments, Nb depletion characteristic of arc environments. The similar geochemistry suggests that the mafic rocks were derived from a similar source and that the dacitic rocks could have been produced by either partial melting or differentiation of the same mafic calcalkaline source. The geochemical coverage is still inadequate to calibrate the Late Triassic calcalkaline stratigraphy of the Hoodoo Mountain area.

The K-feldspar porphyritic, silica undersaturated, volcanic and syenitic rocks form a petrographically and geochemically distinct unit that is associated with skarn and base metal vein mineralization at the Dirk and Telena properties and surrounding area (Chadwick and Close, 2009; Mihalynuk *et al.*, 2011b). These rocks are characterized by Th and LREE enrichment without any appreciable Nb depletion, suggesting that they were derived from an enriched source distinct from the other Late Triassic sources. To the north of the study area, similar rocks have been constrained to be Late Norian (Brown *et al.*, 1996; Logan *et al.*, 2000) and are associated with alkali porphyry mineralization at Galore Creek (*ca.* 210 to 205 Ma; Logan and Koyanagi, 1994; Mortensen *et al.*, 1995). To the east similar aged intrusive rocks underlie the Newmount Lake property (*ca.* 203–214 Ma; Romios Gold Resources Inc., 2008). To the south, similar rocks form part of the latest Triassic alkalic Zippa Mountain pluton (Coulson *et al.*, 1999). Alkalic rocks tend to occur in tectonic settings where undepleted mantle melt can transit the crust relatively unimpeded, such as in rift and post-collisional settings (Richards, 2009). As such, Late Norian to Rhaetian alkalic magmatism in NW Stikinia represents a significant change in the tectonic setting and magma sources from the preceding Late Triassic calcalkalic arc magmatism.

Early Jurassic rocks

The presence of hornblende and plagioclase porphyritic volcanoclastic rocks generally distinguishes the Early Jurassic Hazelton Group from the Late Triassic Stuhini Group volcano-sedimentary rocks in the study area. Trace element geochemistry of the Jurassic tuff and K-feldspar porphyritic rocks indicate that they were formed in a similar arc source to the Triassic volcanic rocks. Hence, the petrography of the Jurassic rocks is the most reliable discriminant from the Triassic strata. In contrast, the petrographically similar Mississippian strata (*e.g.* similar phenocryst assemblages) are geochemically distinct from the Early Jurassic rocks in the Hoodoo Mountain area (Figures 8, 10).

SUMMARY

Mississippian to Pliensbachian volcanic and hypabyssal rocks were analyzed to test the utility of geochemistry to discriminate petrographically similar sequences and to geochemically calibrate the stratigraphy in the Hoodoo Mountain area (NTS 104B/14E). The cross-calibration of stratigraphy and geochemistry also constrains the tectonic and metallogenic evolution of Stikinia and its Jurassic overlap sequences. Our study confirms the utility of geochemistry in stratigraphic calibration and predictive metallogeny. For example, the Mississippian bimodal tholeiitic volcanic sequence is distinct from Late Triassic and Early Jurassic calcalkaline volcanic rocks. Trace element characteristics of these rocks are indicative of VMS-prospective environments consistent with the known VMS-style mineralization in the Iskut (Logan *et al.*, 2000; Logan, 2004; Mihalynuk *et al.*, 2011b) and adjacent areas (Macdonald *et al.*, 1996). The Late Triassic to Early Jurassic calcalkaline sequences display distinct petrographic characteristics (see Logan *et al.*, 2000; Mihalynuk *et al.*, 2011b) that can be utilized in stratigraphic correlations; however, geochemistry appears to have limited use in the discrimination. The alkali volcanic rocks of presumed Norian age are an exception to this caveat. The presence of rhomb porphyries, biotite and chrome diopside geochemical characteristics make these Norian alkali rocks petrographically and geochemically distinct within the predominantly calcalkaline volcanic sequences of the Late Triassic (Logan and Koyanagi, 1994; Mihalynuk *et al.*, 2011b). The frequent association of alkali rocks and Cu-Au mineralization (Logan and Koyanagi, 1994; Romios Gold Resources Inc., 2008; Chadwick and Close, 2009) makes them an important target for mineral exploration in northwestern British Columbia. Ongoing studies in 2012 will follow-up results of the 2011 fieldwork (Mihalynuk *et al.*, 2012) and continue to test the prospectivity of the Hoodoo Mountain area.

ACKNOWLEDGMENTS

This study has been funded through the Geological Survey of Canada GEM initiative (Geological Survey of Canada contribution #20110289), Pacific Northwest Capital and University of Victoria (British Columbia Ministry of Energy, Mines and Resources Partnership Fund). Renaud Soucy la Roche is thanked for his tireless assistance during 2010 field work. Neil Rogers is thanked for detailed and constructive review.

REFERENCES

- Alldrick, D.J., Nelson, J.L. and Barresi, T. (2005): Tracking the Eskay Rift through northern British Columbia: geology and mineral occurrences of the upper Iskut River area; Geological Fieldwork 2004, *BC Ministry of Energy, Mines and Petroleum Resources*, Paper 2005-1, pages 1-30.

- Anderson, R.G. (1993): A Mesozoic stratigraphic and plutonic framework for northwestern Stikinia (Iskut River area), northwestern British Columbia, Canada; in G.C. Dunne and K.A. McDougall (Editors), *Mesozoic paleogeography of the western United States, II; Society of Economic Paleontologists and Mineralogists*, Pacific Section, Los Angeles, CA, pages 477-494.
- Barresi, T. and Dostal, J. (2005): Geochemistry and Petrography of Upper Hazelton Group Volcanics: VHMS-Favourable Stratigraphy in the Iskut River and Telegraph Creek Map Areas, Northwestern British Columbia; Geological Fieldwork 2004, *BC Ministry of Energy, Mines and Petroleum Resources*, Paper 2005-1, pages 39-48.
- Brown, D.A., Gunning, M.H. and Greig, C.J. (1996): The Stikine project: geology of western Telegraph Creek map area, northwestern British Columbia (NTS104G/5, 6, 11W 12 and 13); *BC Ministry of Energy, Mines and Petroleum Resources*, Bulletin 95; 183 pages.
- Cabanis, B. and Lecolle, M. (1989): Le diagramme La/10-Y/15-Nb/8; un outil pour la discrimination des series volcaniques et la mise en evidence des processus de melange et/ou de contamination crustale. The La/10-Y/15-Nb/8 diagram; a tool for distinguishing volcanic series and discovering crustal mixing and/or contamination; *Comptes Rendus de l'Academie des Sciences, Serie 2, Mecanique, Physique, Chimie, Sciences de l'Univers, Sciences de la Terre*, 309(20), pages 2023-2029.
- Chadwick, P. and Close, S. (2009): Geological and geochemical report on the Dirk property, prepared for Romios Gold Resources; *BC Ministry of Energy, Mines and Petroleum Resources*, Assessment Report 31250, 31 pages plus appendices.
- Childe, F., Barrett, T.J. and McGuigan, P.J. (1994): The Granduc VMS deposit, northwestern British Columbia, U-Pb ages and Pb isotope relations; Abstracts with Programs; *Geological Society of America*, 26(7), 381 pages.
- Coulson, I.M., Russell, J.K. and Dipple, G.M. (1999): Origins of the Zippa Mountain Pluton, a Late Triassic, arc-derived, ultrapotassic magma from the Canadian Cordillera; *Canadian Journal of Earth Sciences*, 36(9), pages 1415-1434.
- Gunning, M.H. (1997): Definition and interpretation of Paleozoic volcanic domains, northwestern Stikinia, Iskut River area, British Columbia; *University of Western Ontario*, Canada, 531 pages.
- Henderson, J.R., Kirkham, R.V., Henderson, M.N., Payne, J.G., Wright, T.O. and Wright, R.L. (1992): Stratigraphy and Structure of the Sulphurets Area, British Columbia; in Current Research, Part A, *Geological Survey of Canada*, Paper 92-1A, pages 323-332.
- Kerr, F.A. (1948): Lower Stikine and western Iskut River areas, British Columbia; *Geological Survey of Canada*, Memoir 246, 94 pages.
- Leshner, C.M., Goodwin, A.M., Campbell, I.H. and Gorton, M.P. (1986): Trace-element geochemistry of ore-associated and barren, felsic metavolcanic rocks in the Superior Province, Canada; *Canadian Journal of Earth Sciences*, 23(2), pages 222-237.
- Logan, J. (2004): Preliminary Litho-geochemistry and Polymetallic VHMS Mineralization in Early Devonian and(?) Early Carboniferous Volcanic Rocks, Foremore Property; Geological Fieldwork 2003, *BC Ministry of Energy, Mines and Petroleum Resources*, Paper 2004-1, pages 105-124.
- Logan, J.M., Drobe, J.R. and McClelland, W.C. (2000): Geology of the Forrest Kerr-Mess Creek area, northwestern British Columbia (NTS 104B/10, 15 & 104G/2 & 7W); *BC Ministry of Energy and Mines*, Energy and Minerals Division, Geological Survey Branch, Bulletin 104, 163 pages.
- Logan, J.M. and Koyanagi, V.M. (1994): Geology and mineral deposits of the Galore Creek area (104G/3, 4); *BC Ministry of Energy, Mines and Petroleum Resources*, Bulletin 92, 95 pages.
- Macdonald, A.J., Lewis, P.D., Thompson, J.F.H., Nadaraju, G., Bartsch, R., Bridge, D.J., Rhys, D.A., Roth, T., Kaip, A., Godwin, C.I. and Sinclair, A.J. (1996): Metallogeny of an Early to Middle Jurassic arc, Iskut River area, northwestern British Columbia; *Economic Geology*, 91(6), pages 1098-1147.
- Macdonald, A.J., van der Hayden, P., Lefebvre, D.V. and Alldrick, D.J. (1992): Geochronometry of the Iskut River Area - An update (104A and B); in Geological Fieldwork 1991, *BC Ministry of Energy, Mines and Petroleum Resources*, Paper 1992-1, pages 495-501.
- Mihalynuk, M., Logan, J. and Zagorevski, A. (2011a): East Hoodoo Mountain-Iskut River Geology (NTS 104B/14E, 11NE); *Geological Survey of Canada*, Open File 6739, scale 1:50 000; doi:10.4095/288739.
- Mihalynuk, M., Logan, J., Zagorevski, A. and Joyce, N. (2011b): Geology and mineralization in the Hoodoo Mountain area (NTS 104B/14E); Geological Fieldwork 2010, *BC Ministry of Forests, Mines and Lands*, Paper 2011-1, pages 37-63.
- Mihalynuk, M., Zagorevski, A. and Cordey, F. (2012): Geology of the Hoodoo Mountain area (NTS 104B/14); Geological Fieldwork 2011, *BC Ministry of Forests, Mines and Lands*, Paper 2012-1, this volume.
- Monger, J.W.H. (1977): Upper Paleozoic rocks of the western Canadian Cordillera and their bearing on Cordilleran evolution; *Canadian Journal of Earth Sciences*, 14(8), pages 1832-1859.
- Mortensen, J.K., Ghosh, D.K. and Ferri, F. (1995): U/Pb geochronology of intrusive rocks associated with Cu-Au deposits in the Canadian Cordillera; in T.G. Schroeter (Editor), Porphyry deposits of the Northwestern Cordillera of North America, *Canadian Institute of Mining, Metallurgy and Petroleum*; Special Volume 46, pages 142-158.
- Nadaraju, G. (1993): Triassic-Jurassic Biochronology of the eastern Iskut River map area, northwestern British Columbia; unpublished M.Sc. thesis, *The University of British Columbia*, 268 pages.
- Pearce, J.A. (1996): A user's guide to basalt discrimination diagrams; in D.A. Wyman (Editor), Trace element geochemistry of volcanic rocks: Applications for massive sulphide exploration; *Geological Association of Canada*, Short Course, pages 79-113.
- Pearce, J.A., Harris, N.B.W. and Tindle, A.G. (1984): Trace element discrimination diagrams for the tectonic interpretation of granitic rocks; *Journal of Petrology*, 25(4), pages 956-983.
- Read, P.B., Brown, R.L., Psutka, J.F., Moore, J.M., Journeay, M., Lane, L.S. and Orchard, M.J. (1989): Geology of

- Parts of Snippaker Creek (104B/10), Forrest Kerr Creek (104B/15), Bob Quinn Lake (104B/16), Iskut River (104G/1), and More Creek (104G/2); *Geological Survey of Canada*, Open File 2094.
- Richards, J.P. (2009): Postsubduction porphyry Cu-Au and epithermal Au deposits; products of remelting of subduction-modified lithosphere; *Geology*, 37(3), pages 247-250.
- Romios Gold Resources Inc. (2008): Petrographic and age determinations for intrusives at Romios Gold's Newmont Lake property suggest intrusives are close in age to Galore Creek deposit; Press Release, June 23, 2008; [URL: http://www.romios.com/s/NewsReleases.asp?ReportID=308698&_Type=Press-Release&_Title=Petrographic-and-Age-Determinations-for-Intrusives-at-Romios-Golds-Newmont-...].
- Sun, S.S. and McDonough, W.F. (1989): Chemical and isotopic systematics of oceanic basalts, implications for mantle composition and processes; *Geological Society*, Special Publications 42, pages 313-345.
- Winchester, J.A. and Floyd, P.A. (1977): Geochemical discrimination of different magma series and their differentiation products using immobile elements; *Chemical Geology*, 20(4), pages 325-343.
- Wright, J.V., Smith, A.L. and Self, S. (1980): A working terminology of pyroclastic deposits; *Journal of Volcanology and Geothermal Research*, 8(2-4), 22 pages.
- Zagorevski, A., Mihalynuk, M. and Logan, J. (2011): Tabulated geochemical data of the Hoodoo Mountain area (104B/14E); *Geological Survey of Canada*, Open File 7040, 1 CD-ROM.
- Zagorevski, A., Mihalynuk, M.G., Logan, J.M., Joyce, N. and Friedman, R. (2012): Geochemistry and geochronology of Mississippian to Pliensbachian volcanic and hypabyssal rocks in the Hoodoo Mountain area (NTS 104B/14E); *Mineral Exploration Roundup 2012*, Technical session abstracts.

